Supporting Information

Shalek et al. 10.1073/pnas.0909350107

SI Text

Materials and Methods. ***Reagents.*** Silicon tetrachloride ($SiCl_4$, 99.998%) was purchased from Sigma Aldrich, poly-L-lysine (0.1% w/v aqueous solution), colloidal Au nanoparticles (50 and 100 nm in diameter) and polystyrene spheres (1 micron diameter) from Ted Pella, and Si (111) and (100) wafers from Silicon Valley Microelectronics and Nova Wafer, respectively. Fluorescein, fluorescein diacetate, 3-aminopropyltrimethoxysilane, cystamine, actinomycin-D and streptavidin-Cy3 from Sigma Aldrich, sulfosuccinimidyl 6-(3'-[2-pyridyldithio]-propionamido) hexanoate (Sulfo-LC-SPDP) from Pierce, TNF-α from GenWay, Ac-DEVD-CHO from Biomol, TUNEL apoptosis detection kit from Upstate, and Alexa Flour 488, Alexa Fluor 350 succinimidyl ester (SE), Alexa Fluor 488 succinimidyl ester (SE), Alexa Fluor 546 succinimidyl ester (SE), Alexa Fluor 546 biocytin, Alexa Fluor 488 Histone H1, Alexa Fluor 488 Rabbit Actin, Alexa Fluor 568 Rabbit Actin, Alexa Fluor-labeled secondary antibodies, Qdot 525 ITK™ carboxyl quantum dots, Qdot 585 ITK™ carboxyl quantum dots, Alexa Fluor-labeled and Qdot-labeled IgGs, Alexa Fluor-labeled IgYs, octadecyl rhodamine B chloride, tetramethylrhodamine (TMR) SE, wheat germ agglutinin (WGA) Alexa Fluor 488 conjugate, QSY-7 amine hydrochloride, Vibrant DiD, DAPI, Hoechst 34580, Quant-iT, TO-PRO-3, Trypsin, Tryple Express, 0.4% Trypan blue, culture media, and fetal bovine serum from Invitrogen. 10x Tris-Buffered Saline (TBS) was purchased from VWR. Label-IT Nucleic Acid Labeling Kits (Cy3 and Cy5) were purchased from Mirus Bio. Small interfering RNA (siRNA; described below) and Hyperfect reagent were purchased from Qiagen. An oligonucleotide labeled with TMR (TMR-CACTGTGGTTGGTGTGGTTGG) was synthesized by Bioneer (DaeJeon, Korea). Primary antibodies including chicken anti-neurofilament h, chicken anti-beta-III-tubulin, rabbit antiglial fibrillary acidic protein (GFAP), as well as Annexin V were purchased from Millipore. Additional primary antibodies, mouse anti-vimentin and mouse anti-Nav1.1a (Scn1a), were purchased from Sigma Aldrich. Plasmids utilized include: CMV-eGFP, CMV-mCherry, CMV-dTomato, pTurboGFP-N (Evrogen), pTurboRFP-N (Evrogen), pTurboRFP-mito (Evrogen), pPhi-Yellow-peroxi (Evrogen), pTagGFP2-tubulin (Evrogen), pTagRFP-laminB1 (Evrogen), pTagBFP (Evrogen), and pSUPER.neo+gfp (Oligoengine). 60-mer shRNA oligonucleotides were also obtained from Oligoengine. HeLa S3 cells were obtained from ATCC. Neural progenitor cells and rat hippocampal neurons were purchased from Brain Bits, LLC. Embryonic stem cell-derived human fibroblasts were a kind gift of the Schlaeger lab at the hESC Core Facility, Harvard University. All chemicals were of the highest grade commercially available.

Fluorescent peptide and protein synthesis. Peptides were synthesized on an Apex 396 single-probe fast wash peptide synthesizer (Advanced ChemTech) as previously described (1). For fluorescent protein synthesis, coding sequences of targeted fluorescent proteins were amplified from pTurboRFP-mito as previously described (1).

Control Delivery Experiments. To verify that delivery was not simple diffusion of solution-born molecules, we applied molecules to the culture media at various time points during the cell culture. Cells were cultured on NW substrates with and without molecules adhered to the surface. After cells on the uncoated surfaces were co-incubated for 24 h with molecule-laden media, they were replated, imaged, and compared to cells cultured on molecule-coated NWs (Fig. S6). The addition of molecules to solution was performed at 0 and 45 min. We note that at the first time point (0 min), half the total amount of the molecule that was applied to the NW surface was added to the culture media as the cells were plated. This amount was determined by measuring the percentage of molecule released into solution within the first 45 min using a NanoDrop 2000c Spectrophotometer (Thermo). After 45 min, the following percentages of each molecule were in solution: plasmid DNA – 25%, siRNA – 46%, Protein – 42%, and Peptide – 37%. Thus, we used 50% of each molecule for our 0 minute time point as this value represents a conservative upper bound. We note that adding molecules to solution 3 h after cell plating yielded delivery levels comparable to those seen on flat silicon substrates or glass cover slips.

We performed an additional experiment to examine the effects of adding molecules to solution at the time of cell plating (t = 0 min) as compared to precoating the NWs with them. For this, we used two biomolecules of the same species, but labeled with different fluorophores (either Alexa 546 (siRNA, Protein), Cy3 (plasmid DNA) or Rhodamine (peptide) (magenta) and Alexa 647 (siRNA, Protein, Peptide) or Cy5 (plasmid DNA) (*Yellow*)), in parallel (Fig. S6*A*). When the NWs were precoated with a mixture of the two molecules, both were efficiently delivered (Fig S6 *A*, top row); when one was applied to the NWs and the other in solution (as above), only the species precoated onto the wires was delivered effectively (Fig S6 *A*, bottom row). This result clearly suggests that the NWs deliver molecules by carrying them across the cell membrane and subsequently releasing them rather than opening transient pores through which molecules in solution can diffuse.

The relative fluorescence (ΔF) was quantified by dividing the average fluorescence intensity in the cells (determined by colocalization with a membrane label, fluorescein diacetate) by the average fluorescence intensity outside the cells, and subtracting from this value from the same quantity measured on a control set of cells. As a control, we cultured cells on top of both flat Si wafer without NWs and glass coverslips and added the molecules to the culture media. The resulting fluorescence was then normalized to the maximum value for each molecule respectively (F_{max}), and plotted in Fig. S6 *B*.

Electrophysiological recording parameters. During the recordings, the Si NW substrates were bathed in a solution containing [in mM]: NaCl [119], KCl [5], HEPES [20], $CaCl_2$ [2], $MgCl_2$ [2], glucose [30], glycine [0.001], pH 7.3, osmolarity adjusted to 330 mosM with sucrose; patch pipettes, pulled to have resistances of ~5 MOhms, were backfilled with a solution containing [in mM]: Potassium Gluconate [130], KCl [10], $MgCl_2$ [5], EGTA [0.6], HEPES [5], $CaCl_2$ [0.06], Mg-ATP [2], GTP [0.2], leupeptine [0.2], phosphocreatine [20], creatine phosphokinase [50 U/ml], pH 7.2 (2). For certain experiments, an acetone stock of 15 mg/ml of fluorescein diacetate, or 1 mg/mL of octadecyl rhodamine b in ethanol, was diluted 1:1000 into the intracellular recording solution to create a fluorescently identifiable patch pipette. All recordings were made at RT with a Multiclamp 700B (Molecular Devices). For voltage clamp experiments, cells were held at -80 mV and currents were recorded in response to a series of hyperpolarizing and depolarizing voltage pulses made in 15 mV increments. For current clamp recordings, current was injected to achieve a resting membrane potential of approximately -75 mV, and cellular responses to test pulses of current were then

recorded. Pipette capacitance was corrected electronically. For voltage clamp recordings, P/N 4 subtraction was used to remove capacitive and leak currents. All acquisitions were performed using pClamp 10 software (Molecular Devices) and plotted using IGOR (WaveMetrics).

Cell Viability upon NW Penetration. Following their initial plating on the Si NW substrates, HeLa cells grew at a slightly slower rate than those on flat silicon. An Annexin V binding assay of NW-impaled HeLa cells consistently showed surface exposure of phosphatidylserine in 10–20% of the cells as they proliferated (Fig. S4*A*–*C*).

Despite slower division rates, and in contrast to a recent report which suggested that Si NWs, particularly in suspensions, exert cytotoxic effects on some cells (3), the NW-impaled cells appeared healthy; nuclear staining tests proved that the Si NWs did not adversely affect the viability of the various cells, including HeLa cells, primary hippocampal neurons, and neurospheres, cultured on top of them for more than one week. Similarly, human fibroblasts plated on both Si NWs and flat silicon were unstained when incubated in an equal parts mixture of 0.4% Trypan blue and culture media for 15 min 1 day after plating, verifying membrane integrity (Fig. S4*E* and *F*).

RNA extraction and quantitative real-time PCR analysis. HeLa S3 and human fibroblast cells were cultured on multiwell plates, flat silicon, or Si NWs for 24 h. Total cellular RNA was isolated using a QIAGEN RNeasy Mini Kit (QIAGEN) according to the manufacturer's instructions. Quantitative mRNA expression analysis of five housekeeping genes was performed using SYBR-Green based quantitative PCR technique (SA Biosciences) according to the manufacturer's instructions. Briefly, one microgram of total RNA was reverse transcribed into first strand cDNA, using an RT† First Strand Kit (SA Biosciences). The resulting cDNA was subjected to quantitative real-time PCR using human gene-specific primers for five different genes (4) (ß-actin (ACTB; Accession #: NM_001101.2; Amplicon length: 233 bp; Primers: Forward (5'-3') – GGACTTCGAGCAAGAGATGG & Reverse (5'-3') – AGCACTGTGTTGGCGTACAG), ß-2-microglobulin (B2M; Accession #: NM_004048.2; Amplicon length: 87 bp; Primers: Forward (5'-3') – TGCTGTCTCCATGTTTGATGTATCT & Reverse (5'-3') – TCTCTGCTCCCCACCTCTAAGT), glyceraldehyde 3-phosphate dehydrogenase (GAPDH; Accession #: NM_002046.2; Amplicon length: 238 bp; Primers: Forward (5'-3') – GAGTCAACGGATTTGGTCGT & Reverse (5'-3') – TTGATTTTGGAGGGATCTCG), ß-glucuronidase (GUSB; Accession #: NM_000181.1; Amplicon length: 171 bp; Primers: Forward (5'-3') – AAACGATTGCAGGGTTTCAC & Reverse (5'-3') – CTCTCGTCGGTGACTGTTCA), and hypoxanthine phosphoribosyltransferase 1 (HPRT1; Accession #: NM_000194.1; Amplicon length: 94 bp; Primers: Forward (5'-3') – TGACACTGGCAAAACAATGCA & Reverse (5'-3') – GGTCCTTTTCACCAGCAAGCT)) and a control 18SrRNA gene (18SrRNA; SA Biosciences product: PPH05666E). The quantitative real-time PCR reaction was performed with an initial denaturation step of 10 min at 95 °C, followed by 15 seconds at 95 °C, and 60 seconds at 60 °C for 40 cycles on an Mx3000P™ QPCR system (Stratagene).

The mRNA expression for each gene, normalized to the 18SrRNA control, was compared among the three samples according to the $2-\Delta\Delta$CT method (5). The results for human fibroblast and HeLa cells are plotted in Fig. S4*D*.

Similarly, quantitative mRNA expression analysis of vimentin knockdown was performed using human gene-specific primers for vimentin (VIM; accession number: NM_000194.1; Qiagen product: QT00095795), ß-actin (ACTB; accession number: NM_001101.2; Qiagen product: QT00095431), and glyceraldehyde 3-phosphate dehydrogenase (GAPDH; Accession number: NM_002046.2; Qiagen product: QT00079247) and a control 18SrRNA gene (SA Biosciences product: PPH05666E). For these runs, mRNA was extracted from HeLa S3 cells to which either no siRNA, AllStar negative siRNA, or pooled siRNAs targeting vimentin had been administered using either the substrate's surface (flat silicon or Si NWs) or a conventional reagent (Hyperfect, Qiagen) 48 h after plating. The mRNA expression for vimentin, normalized to either the listed housekeeping genes or the 18SrRNA control, was compared to siRNA-free and AllStar negative controls for each of the samples according to the $2-\Delta\Delta$ CT method (5). Si NW samples showed substantial vimentin knockdown when the siRNA was administered using the NWs or a conventional reagent, while flat silicon samples only showed knockdown when a conventional reagent was used (Fig. S8).

Efficiency of Biomolecule Delivery. To assess the efficiency of delivery for each molecule of interest, the fraction of cells containing that molecule were counted. For each molecule tested, the number of cells counted and the efficiencies were: Rhodamine (cells counted: 421, efficiency: 99.3%), AllStar siRNA Alexa Fluor 546 (cells counted: 152, efficiency: 99.3%), GNU siRNA Alexa Fluor 546 (cells counted: 427, efficiency: 99.8%), Rhodamine-labeled 7-mer peptides (cells counted: 224, efficiency: 99.5%), Cy5-DNA (cells counted: 365, efficiency: 100%), QD 585 labeled IgG (cells counted: 165, efficiency: 95.8%), TurboRFP-Mito (cells counted: 461, efficiency: 99.3%), and Anti-Vim Cy3 (cells counted: 33, efficiency: 100%).

Immunostaining. Samples were fixed in 4% formaldehyde in PBS (RT, 20 min), permeabilized in 0.25% triton-x 100 in PBS (RT, 10 min), and blocked in 10% goat serum in PBS (RT, 1 hour). After washing with PBS, primary antibodies against the relevant proteins (chicken anti-neurofilament h, chicken anti-beta-III-tubulin, rabbit anti-glial fibrillary acidic protein (GFAP), mouse anti-vimentin, and/or mouse anti-$Na_v1.1a$ (Scn1a)) were added to 5% goat serum in PBS at a 1:250 dilution and the samples were rocked overnight at 4 °C. The samples were then washed with PBS and incubated with Alexa Fluor labeled secondary antibodies (1:500 dilution) in 2.5% goat serum (1 hour, RT). After washing with PBS, they were imaged with an upright microscope (Olympus) and a mercury lamp (EXFO). For some samples, prior to imaging, nuclei were counterstained by incubating the substrates with 300 ng/mL of DAPI in PBS or 1 mM TO-PRO-3 in PBS (RT, 30 min).

Construction of short hairpin RNA (shRNA) plasmid. 60-mer shRNA oligonucleotides sequences for the targeted genes were made to contain 19-nucleotide sense and antisense regions, linked by a short hairpin. The sense sequences used were: $Na_v1.X$ (targeted against rat fast inward sodium channels $Na_v1.1$ (Scn1a), $Na_v1.2$ (Scn2a1), $Na_v1.3$ (Scn3a), and $Na_v1.9$ (Scn9a)): 5'-GTTCGACCCTGACGCCACT-'3; GNU (targeted against the *Drosophila Melanogaster* gene GNU): 5'-CTACTGAGAACTAAGAGAG-'3 (6). Forward and reverse strands for each gene were annealed and subcloned into pSUPER.neo+gfp plasmids following the manufacturer's instructions. Before use, all constructs were verified by sequencing at the Dana-Farber/Harvard Cancer Center DNA Resource Core.

shRNA knockdown of gene expression. Since rat hippocampal neurons grown on Si NWs display typical electrophysiological signatures (e.g., action potentials) after one week of culture, we attempted to knockdown this behavior by using the aforementioned shRNA constructs to interfere with normal expression of multiple sodium channel subtypes. Eight days after being plated on NWs laced with those constructs, rat hippocampal neurons

were examined for eGFP, and hence shRNA, expression (Fig. S3*A*). Upon identifying fluorescent cells, whole-cell patch clamp recordings were made. In voltage clamp, neurons transfected with $pNa_v1.X$ did not display the large, fast, inward sodium currents that normally underlie action potential generation in response to depolarizing voltage steps that the pGNU transfected cells did (Fig. S3*B* to *D*). Similarly, in current clamp, $pNa_{v1}1.X$ neurons did not spike when subjected to the depolarizing current pulses that evoked action potentials in pGNU neurons (Fig. S3*E*–*H*).

Apoptosis assay. TUNEL staining was performed using the apoptosis detection kit according to the manufacturer's instructions with minor modifications. Briefly, after treatment with actinomycin-D and TNF-α, the cells on the Si NWs were washed in PBS and fixing with 4% paraformaldehyde in PBS (RT, 15 min). Following a wash with PBS, the cell-containing Si NWs were incubated in PBS containing 0.5% Tween-20 and 0.2% BSA (RT, 15 min). Freshly prepared TdT end-labeling cocktail (made by mixing TdT buffer, biotin-dUTP, and TdT at a ratio of 18:1:1) was then added to the cell-containing Si NWs. After 1 hour incubation at RT, the reaction was stopped by removing the TdTend-labeling cocktail and immersing samples in TB buffer (RT, 5 min). A blocking buffer was then applied to the Si NWs (RT, 20 min). Finally, streptavidin-Cy3 (20 μg/mL) and WGA Alexa Fluor 488 (50 μg/mL) were then incubated with the samples (RT, 30 min) before examining them under a fluorescence microscope.

For the Annexin V staining, the Si NWs samples, treated with actinomycin-D and TNF-α, were washed in PBS and binding buffer (10 mM HEPES, 140 mM NaCl, 2.5 mM $CaCl_2$, pH 7.4). After incubating the samples with Annexin V-FITC at 1 μg/mL (RT, 15 min), the cells were washed in excess binding buffer and analyzed by fluorescence microscopy.

1. Stiffler MA, Grantcharova VP, Sevecka M, MacBeath G (2006) Uncovering Quantitative Protein Interaction Networks for Mouse PDZ Domains Using Protein Microarrays. *J Am Chem Soc* 128(17):5913–5922.
2. Arancio O, Kandel ER, Hawkins RD (1995) Activity-dependent long-term enhancement of transmitter release by presynaptic 3′,5′-cyclic GMP in cultured hippocampal neurons. *Nature* 376(6535):74–80.
3. Qi S et al. (2007) Effects of Silicon Nanowires on HepG2 Cell Adhesion and Spreading. *ChemBio Chem* 8(10):1115–1118.
4. Ionescu-Zanetti C et al. (2005) Mammalian electrophysiology on a microfluidic platform. *Proc Natl Acad Sci USA* 102(26):9112–9117.
5. Livak KJ, Schmittgen TD (2001) Analysis of relative gene expression data using real-time quantitative PCR and the 2(-Delta Delta C(T)) Method. *Methods* 25(4):408, 402–408, 402.
6. Xu X, Shrager P (2005) Dependence of axon initial segment formation on Na+ channel expression. *J Neurosci Res* 79(4):428–441.

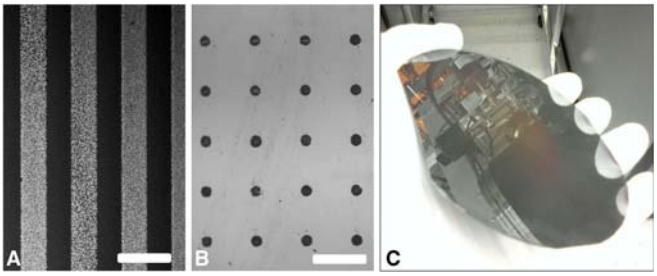

Fig. S1. Silicon NW fabrication is controllable and scalable. (*A*) and (*B*) Grown Si NWs patterned to form lines and circles respectively. Patterns were generated by either flowing the gold nanoparticles that catalyzed the CVD growth of the NWs through PDMS microfluidic channels (*A*) or stamping those particles with patterned PDMS stamps (*B*). Scale bar, 200 μm. (*C*) Photograph of a typical 4″ diameter wafer uniformly covered with etched Si NWs.

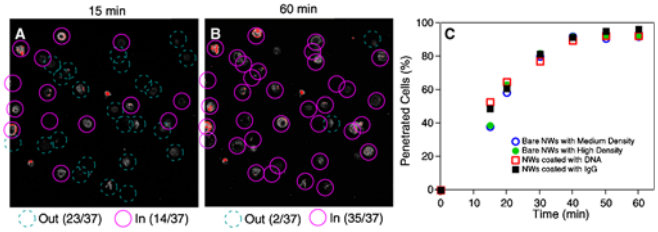

Fig. S2. The kinetics of Si NW penetration are not affected by the nature of the molecule attached to the wires. (*A*) and (*B*) Confocal images of membrane-labeled HeLa cells 15 and 60 min after plating, respectively. Dashed circles surround cells that sit atop the wires as indicated by the absence of a fluorescent annulus (Fig. 1*C* and *E*). Solid circles surround cells which have been penetrated as in Fig. 1*D* and *F*. (*C*) Percentage of cells penetrated as a function of time after plating as determined by confocal images such as those in *A* and *B*. Shapes represent different NW conditions as shown in the legend. NW coating shows no measurable effect on the kinetics of penetration.

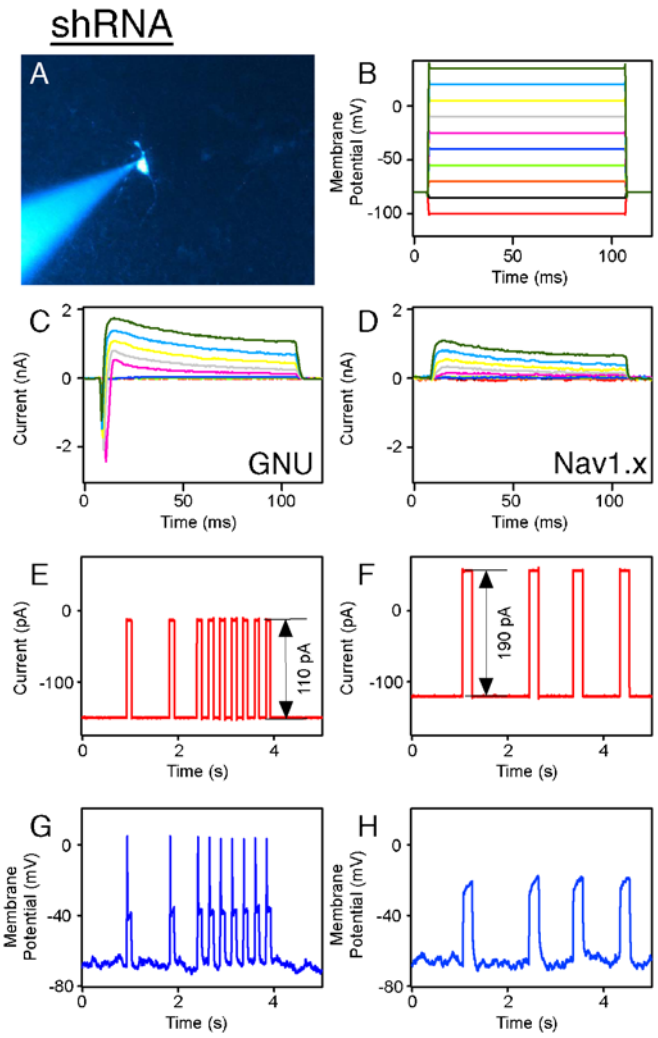

Fig. S3. Knockdown of fast, inward sodium currents in rat hippocampal neurons via delivery of an shRNA and eGFP encoding plasmid. (*A*) Fluorescence image showing the patch clamping of an eGFP, and hence shRNA, expressing 8 DIV neuron. (*B*) Applied hyper- and de-polarizing voltage steps. (*C*) and (*D*) Current responses of a neuron transfected with a control plasmid (pGNU) and one with shRNAs targeted against sodium channels (pNa$_v$1.X), respectively. Panel *C* displays fast, inward voltage gated sodium currents and outward delayed-rectifier potassium currents while *D* only shows the latter. (*E*)B (*H*) Current clamp recordings of those samples' neurons show that while pGNU transfected cells fire action potentials (*G*) upon current injection (*E*), pNa$_v$1.X cells do not (*H* and *F*, respectively).

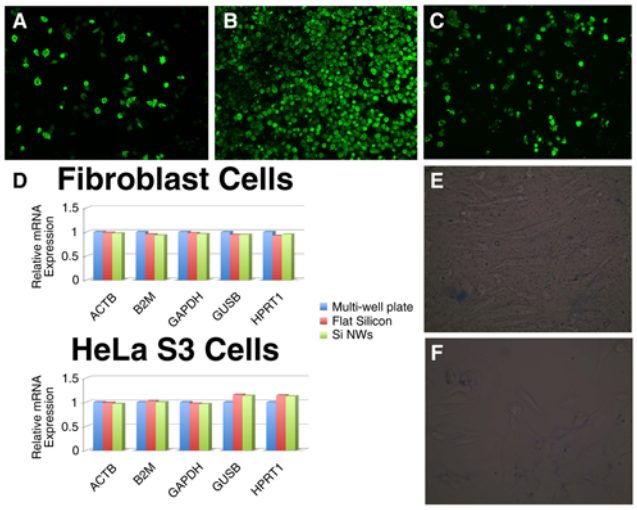

Fig. S4. Health of NW-penetrated cells. (*A*) to (*C*): Annexin V assay of HeLa cell cultures on Si NWs. (*A*) Cells on flat Si NWs. (*B*) Cells on flat Si NWs treated with actinomycin-D (1 μg/mL) for 30 min, followed by incubation with TNF-a (2 ng/mL) for 7 h. (*C*) Cells on Ac-DEVD-CHO-coated Si NWs treated with actinomycin-D and TNF-a. (*D*): Si NW penetration mimimally perturbs cells. (*D*) Relative mRNA expression, as determined by real-time PCR, for both human fibroblast and HeLa S3 cells. Five housekeeping genes show similar expression levels for cells plated on Si NWs, flat silicon, and conventional multiwell plates. (*E*) and (*F*): Trypan blue (a membrane impermanent dye) does not stain NW-pentrated cells. Cells plated on Si NW (*E*) or flat silicon (*F*) do not show appreciable staining after being incubated for 15 min in a solution made of equal parts of 0.4% Trypan blue and cell culture media. This indicates the integrity of the cellular membranes of cells cultured on both Si NW and flat silicon.

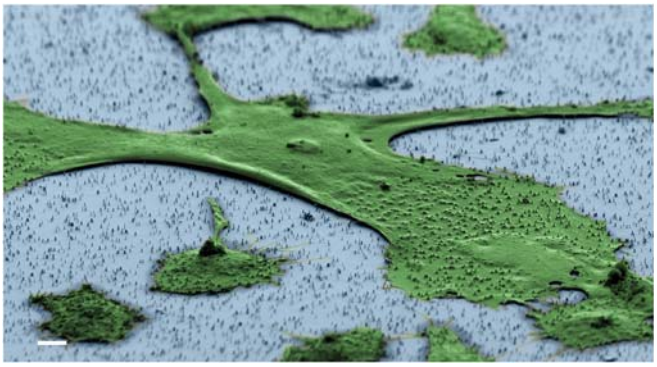

Fig. S5. Scanning electron micrograph of human fibroblasts (one day after plating: false colored green) atop an array of etched Si NWs (false colored blue). Scale bar, 10 μm.

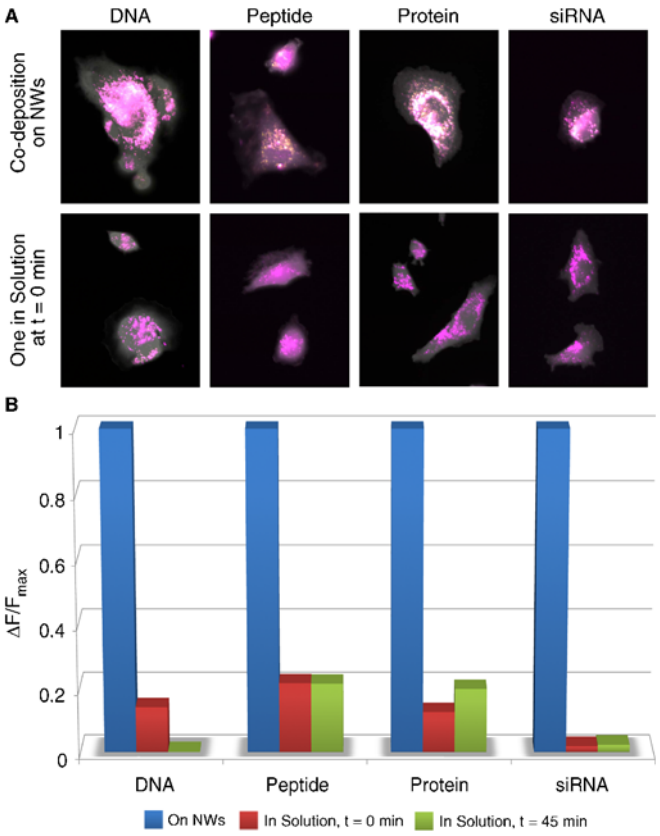

Fig. S6. Relative fluorescence intensity of various molecules delivered to human fibroblasts via Si NWs. (*A*) By delivering two biomolecules of the same species, but labeled with different fluorophores, in parallel, the contribution of solution-based delivery through pores temporarily opened by the NWs was examined. When the NWs were precoated with a mixture of the two molecules, both were efficiently delivered (*Magenta* and *Yellow*); when one was applied to the NWs (*Magenta*) and the other in solution (*Yellow*), only the species precoated onto the wires (*Magenta*) was delivered effectively. (*B*) In separate experiments, molecules were added on the NW surface before cells were plated, or to the solution at different time points (at plating and 45 min after plating). 24 h after plating, several fluorescence images were taken of the cells after removal from the Si NW substrate. The difference between the average fluorescence of cells plated on NWs and control cells (ΔF) was then normalized to the maximum fluorescence measured for each molecule respectively. Reduced delivery of molecules administered in solution indicates that diffusion of free floating molecules across the cell membrane or through membrane pores, is not the primary mechanism for delivery.

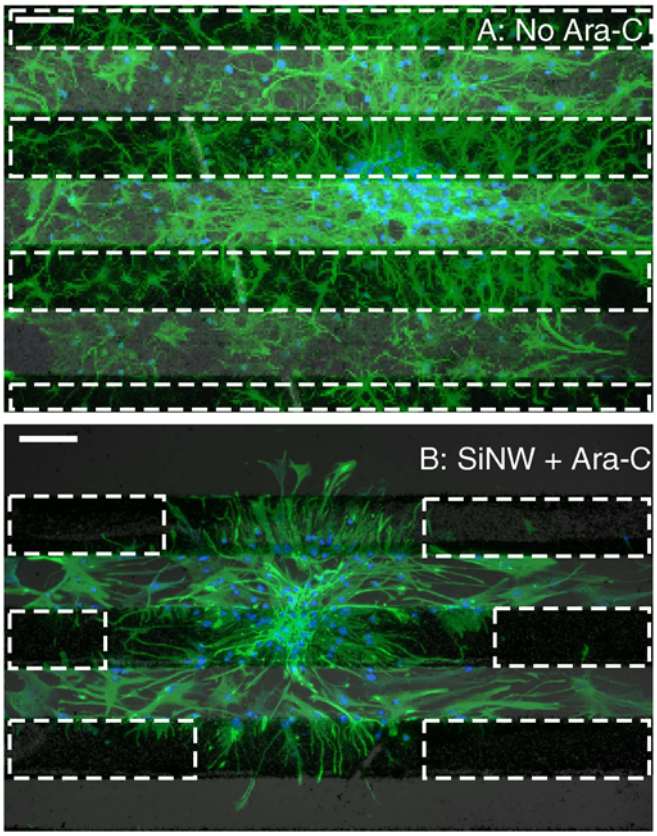

Fig. S7. Patterned NWs can selectively influence cellular phenomena. (*A*) and (*B*) Rat neural progenitor cells plated atop patterned stripes of Si NWs. The substrate in (*B*) has been blanket coated with the mitotic inhibitor Ara-C while the substrate in (*A*) has not. (*A*) NPCs plated on a line-patterned Si NW substrate in the absence of Ara-C divide out isotropically from their point of plating. (*B*) shows that cell division is selectively stopped as cells enter or cross regions where the Si NWs deliver Ara-C (*Dashed rectangles*). Scale bar, 100 μm.

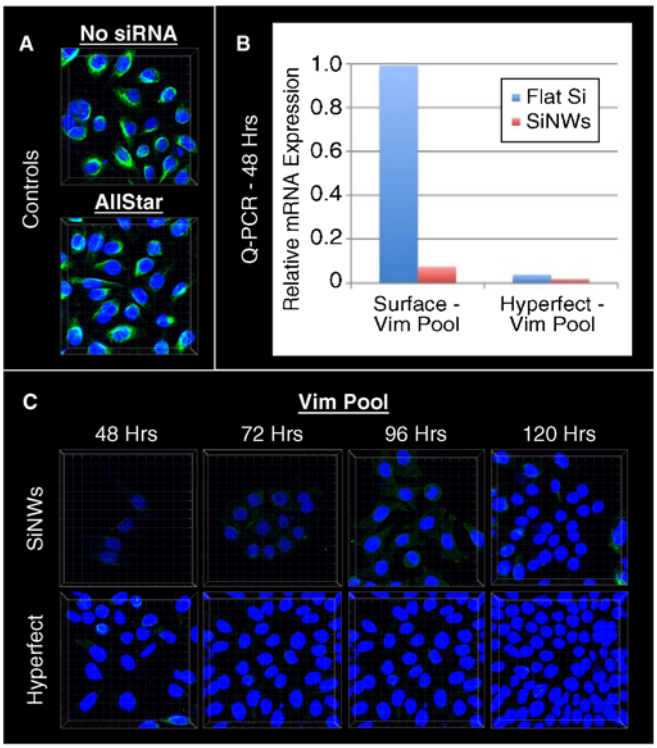

Fig. S8. Stability and efficacy of siRNA delivered via Si NW versus Hyperfect (conventional reagent). (*A*) Confocal scans of HeLa S3 cells (nuclei in blue) immunostained for vimentin (*Green*). At 72 h, HeLa S3 cells plated on Si NWs either untreated or treated with AllStar negative control siRNA show no vimentin (*Green*) knockdown. (*B*) 48 h after plating, real time-PCR shows that siRNA delivered via Si NWs or a conventional reagent, Hyperfect, efficiently knocks down vimentin as compared to control samples (no siRNA). Coating silanized flat silicon with vimentin-targeting pooled siRNAs does not lead to an appreciable amount of vimentin knockdown. (*C*) Confocal scans, as in (*A*), showing the degree of vimentin knockdown achieved by administering pooled siRNAs with Si NWs or a conventional reagent at 48, 72, 96, and 120 h after administration. Both techniques show similar stability; at all time points, substantial knockdown is seen regardless of whether a conventional reagent or Si NWs are used. Field of view for all confocal images is $140 \times 140\ \mu m$

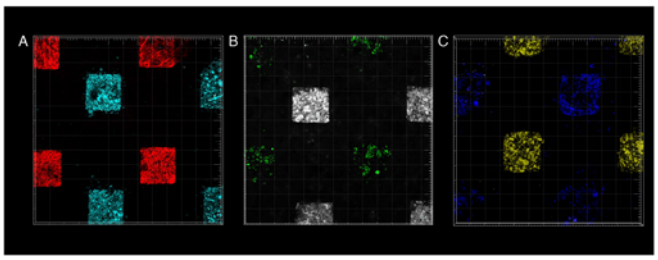

Fig. S9. Additional examples of site-specific delivery. (*A*) Directed introduction of two different Alexa Fluor (488-cyan and 568-red) labeled rabbit actins. (*B*) Patterned delivery of two different proteins, an Alexa Fluor 488 labeled histone H1 (*Green*) and an Alexa Fluor 568 labeled actin (*White*). Note that the distribution of the two proteins is markedly different. (*C*) A second example of targeted siRNA (*Yellow*) and histone (*Blue*) delivery. All images were taken one day after plating cells. Field of view for all images is $635 \times 635\ \mu m$.